arXiv:cond-mat/0210165v2 [cond-mat.soft] 29 May 2003

External and intrinsic anchoring in nematic liquid crystals: A Monte Carlo study

N. V. Priezjev,[1] G. Skačej,[2] R. A. Pelcovits,[1] and S. Žumer[2]

[1]*Department of Physics, Brown University, Providence, Rhode Island 02912*

[2]*Department of Physics, University of Ljubljana,*

Jadranska 19, SI-1000 Ljubljana, Slovenia

(Dated: December 29, 2021)

Abstract

We present a Monte Carlo study of external surface anchoring in nematic cells with partially disordered solid substrates, as well as of intrinsic anchoring at free nematic interfaces. The simulations are based on the simple hexagonal lattice model with a spatially anisotropic intermolecular potential. We estimate the corresponding extrapolation length b by imposing an elastic deformation in a hybrid cell-like nematic sample. Our estimates for b increase with increasing surface disorder and are essentially temperature–independent. Experimental values of b are approached only when both the coupling of nematic molecules with the substrate and the anisotropy of nematic–nematic interactions are weak.

PACS numbers: 61.30.Cz, 61.30.Gd

I. INTRODUCTION

In confined nematic liquid crystals with a large surface–to–volume ratio the aligning effects of the confining surfaces are of great importance in determining the equilibrium director configuration [1]. There are two major contributions to these surface aligning effects, the first one originating from direct interactions between nematic molecules and the solid substrate (external anchoring), while the second one is due to incomplete anisotropic nematic-nematic interactions in the vicinity of the sample surface (intrinsic anchoring). An understanding of these confinement related aligning mechanisms is of great importance not only from the fundamental point of view, but also, e.g., for the design and construction of liquid crystal–based optical devices. Within phenomenological approaches anchoring effects are usually characterized by two parameters: the preferred molecular alignment direction at the sample surface (the easy axis) and the free energy coefficient W penalizing any deviation from this direction (the anchoring strength) [2]. Here the W coefficient depends on S, the nematic order parameter. This dependence seems to be strongly related to the specific properties of a given interface: for example, for a system of hard rods confined between hard walls one finds $W \propto S$ [3], while in experiments measuring anchoring inside polycarbonate membranes even $W \propto S^4$ can be obtained [4]. Given, moreover, $K \propto S^2$ [5, 6] (K denoting the Frank elastic constant), with decreasing S the extrapolation length $b = K/W$ [5] may either increase (as seen experimentally in thermotropics [4]), or decrease (as obtained from simulations with hard particles [7]). In the bulk, the value of S is primarily determined by temperature, while close to an interface it may also be affected by incomplete bulk interactions, as well as by (dis)ordering effects of the (possibly rough) confining substrate. In the latter case W is often assumed to be simply proportional to $\mathcal{W}S_0S(0)$, where $\mathcal{W}$ represents the surface coupling constant, S_0 the surface–imposed value of S (determined by substrate roughness), and $S(0)$ its actual surface value [8].

While both the anchoring strength and the easy axis can be determined experimentally [9], it is also possible to deduce them from simulations based on pairwise intermolecular interactions. For example, intrinsic anchoring has been analyzed in a pseudomolecular continuum approach with ellipsoidal molecules [10], using a lattice approximation in the zero–temperature limit [11], or analyzing different types of interfaces in Gay–Berne systems [12, 13, 14]. Furthermore, surface anchoring strength has also been measured in a

system of hard ellipsoids in contact with a hard wall [7, 15]. The anchoring strength reported in most analyses shows that anchoring is rather strong and that the corresponding extrapolation length is of the order of a few molecular dimensions, while its experimental values are typically above 100 nm [9]. On the other hand, a recent analysis of external anchoring — also based on a lattice model, but for nonzero temperature — was presented in Ref. [16], showing that the extrapolation length can increase significantly when the nematic–to–isotropic (NI) transition is approached, as also seen experimentally [4]. Moreover, a lattice gas approach has been adapted recently to study nematic interfaces [17].

Motivated by these developments, in this paper we extend the analyses performed in Refs. [11, 16] to nonzero temperatures (employing Monte Carlo simulations) and repeat the measurement of the extrapolation length both for external and intrinsic anchoring, the former in presence of rough solid substrates and the latter for a free nematic interface. The term "rough" here refers to flat but partially disordered substrates. We will first briefly recall the features of the lattice model used in Ref. [11], then discuss the modifications needed to perform the present analysis, and finally, present and discuss the results.

II. SIMULATION MODEL AND ANCHORING MEASUREMENT

We model a liquid crystalline slab of thickness d, using a modification of the well–known Lebwohl–Lasher (LL) model [18]. In the LL model elongated nematic molecules are represented by freely-rotating spin-like particles that are attached to lattice points of a cubic lattice. Since the pairwise interaction energy used in the LL model is spatially isotropic and thus does not depend on the relative position of the particles, it cannot produce any orienting effects at a free nematic surface and is therefore not suitable for studies of intrinsic anchoring. Therefore, we choose a more general potential to model the interparticle interaction energy resulting from anisotropic van der Waals forces. These forces can give rise to the nematic phase [19] even without hard rod repulsion. For two neighboring nematic particles i and j with orientations given by unit vectors $\mathbf{u}_i$ and $\mathbf{u}_j$, separated by $\mathbf{r}_{ij}$, we model the interaction potential as [20]:

$$U_{ij} = -\epsilon \left[\mathbf{u}_i \cdot \mathbf{u}_j - 3\nu (\mathbf{u}_i \cdot \frac{\mathbf{r}_{ij}}{r_{ij}})(\mathbf{u}_j \cdot \frac{\mathbf{r}_{ij}}{r_{ij}}) \right]^2 \tag{1}$$

with $\epsilon > 0$, which for $\nu = 0$ reduces to the standard LL potential, while for $\nu = 1$ one has the induced dipole-induced dipole interaction. The spatial anisotropy parameter ν enables us to continuously vary the relative importance of the spatially anisotropic ($\mathbf{r}_{ij}$-dependent) contribution to the interaction law (1). Although the range of van der Waals potential is proportional to r_{ij}^{-6}, for computational efficiency we consider only interactions between nearest neighbors. Thereby the intrinsic anchoring energy W and the elastic constant K are underestimated, but we expect the errors in the estimation of W and of the extrapolation length K/W not to exceed 20% and 30%, respectively.

In a nematic slab, boundary conditions are typically fixed by the interaction with solid walls, or, alternatively, through orienting effects near free nematic interfaces. In the simulation, each of the solid walls is represented by a layer of fixed particles $\mathbf{p}_i$ ($|\mathbf{p}_i| = 1$), either all perfectly aligned or somewhat disordered with some residual order. The nematic–wall interaction is modeled via

$$U_{ij}^{s} = -\epsilon_s \left[\mathbf{p}_i \cdot \mathbf{u}_j\right]^2, \tag{2}$$

as promoted, e.g., by short–range steric forces, where, again, $\mathbf{p}_i$ and $\mathbf{u}_j$ are nearest neighbors on the lattice. A dimensionless anchoring strength parameter can be defined as $w = \epsilon_s/\epsilon$. In the case of a perfectly aligned surface one has $\mathbf{p}_i = \mathbf{\Pi}$, i.e., all particles are aligned along the easy axis $\mathbf{\Pi}$, while for disordered surfaces $\mathbf{\Pi}$ represents the average orientation of $\mathbf{p}_i$. On the other hand, a free nematic interface is simply modeled through the missing–neighbor effect.

Instead of the cubic lattice used in the LL model, in present simulations we use a simple hexagonal lattice to model the liquid crystal, which is necessary to avoid unphysical bulk easy axes [11] for $\nu \neq 0$. These axes arise as a direct consequence of using a lattice approximation for modeling an anisotropic liquid and are present for any spatially anisotropic potential in the cubic lattice. They are absent, however, in the hexagonal lattice, provided that the spins $\mathbf{u}_i$ are assumed to be two–dimensional vectors confined to hexagonal planes. The geometry of our sample is shown in Fig. 1. The z axis is normal to the confining interfaces and the hexagonal planes are parallel to the xz plane. We stress that our analysis must be restricted to low values of the anisotropy parameter ν in order to avoid solid-like periodic director profile solutions that are stable for $\nu > 0.3$ [11].

The strength of any anchoring can be measured by imposing an elastic distortion so that

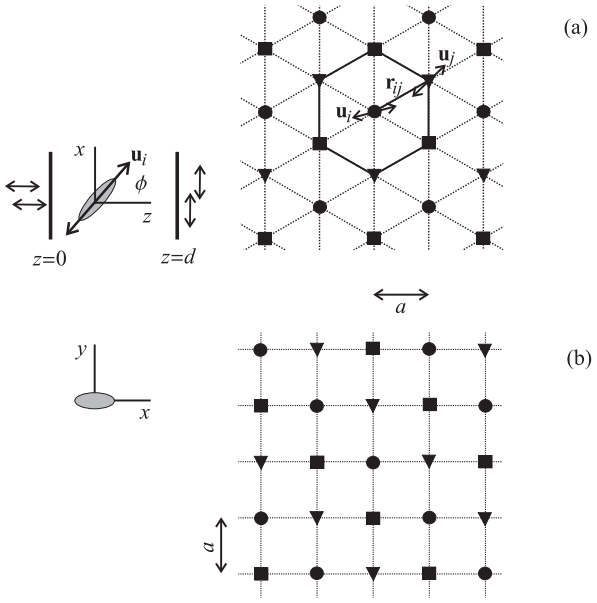


FIG. 1: Sample geometry, hexagonal lattice and the three sublattices (squares, circles, and triangles): (a) xz and (b) xy cross sections. The tilt angle $\phi = \phi(z)$ is measured with respect to the z-axis, the sample normal. Boundary conditions at $z = 0$ and $z = d$ are homeotropic and planar, respectively.

the average surface molecular orientation deviates from the easy axis defined by the anchoring. The magnitude of this deviation can then be used to estimate the anchoring strength and the corresponding extrapolation length [5]. The elastic distortion in a nematic slab can be imposed either by applying a magnetic field whose orientation must not coincide with the direction of the easy axis, or by antagonistic anchoring conditions at opposing surfaces. In the zero-temperature analysis of Ref. [11] the magnetic field method was used. On the other hand, for nonzero temperatures a strong enough magnetic field can enhance the degree of nematic order and even shift the NI phase transition, which can present additional difficulties in interpreting the results. Therefore, we decided not to use the magnetic field approach; instead, we consider a hybrid cell-like sample with antagonistic boundary conditions.

Consider the $\nu = 0$ case with pure external anchoring first. The left ($z = 0$) interface — where the anchoring will be measured — is chosen to be a solid wall, either perfectly ordered or somewhat disordered, promoting homeotropic alignment through weak external

anchoring ($w = 0.1$). At the same time, the right ($z = d$) interface is also taken to be a solid wall, yet with perfect planar alignment and strong external anchoring ($w = 1$). For the case $\nu \neq 0$, we replace the solid wall at $z = 0$ with a free nematic interface, enabling us to study intrinsic anchoring alone. Note that for $\nu \leq 0.3$ the easy axis of the free interface is homeotropic [11], thus providing the same confinement type as with external anchoring. As a result, in both cases a combined bend and splay elastic deformation is expected to appear in the sample. The deformation should be present as long as the sample thickness d exceeds $d_c = |(K/W)_0 - (K/W)_d|$, where $(K/W)_0$ and $(K/W)_d$ are the extrapolation lengths corresponding to the effective anchoring on the left and the right wall, respectively, while for $d < d_c$ a uniform director structure is observed [21]. In a hybrid cell close to NI transition a non-bent biaxial structure is also possible, consisting of two strata of uniform alignment, separated by a biaxially ordered layer [22]. Recall that unlike in the original LL model in the present study spins $\mathbf{u}_i$ are two–dimensional vectors and hence unable to reproduce biaxiality.

For hybrid boundary conditions in the one–constant approximation the Frank elastic theory (assuming a constant degree of nematic order throughout the slab) predicts a perfectly linear director tilt angle profile $\phi(z)$, where ϕ is measured, e.g., with respect to the slab normal z. The torque balance condition at, e.g., the left surface ($z = 0$) can be written as $(d\phi/dz)_0 = \frac{1}{2}(W/K)_0 \sin 2\phi(0)$ and enables us to deduce $(K/W)_0$ from the measured values of $(d\phi/dz)_0$ and $\phi(0)$. Note that for small $\phi(0)$ (i.e., strong enough anchoring) the above condition simplifies to $(d\phi/dz)_0 = (W/K)_0\phi(0)$ and allows us to determine $(K/W)_0$ simply by extrapolating the profile $\phi(z)$ graphically across the sample boundary to $\phi = 0$ corresponding to the homeotropic easy axis. Note also that if the degree of nematic order is subject to variations — which is usually the case near sample boundaries in a layer of thickness ξ (ξ denoting the nematic correlation length) — the profile $\phi(z)$ may deviate from the above predicted linear behavior. In this case the extrapolation of the profile towards the surface must be performed from far enough in the bulk where the order parameter profile is constant, that is from $\xi < z < d - \xi$. Note also that whenever $(K/W)_0$ approaches d (for weak anchoring or in a thin sample), $(d\phi/dz)_0$ and, consequently, $(K/W)_0$ are accompanied by a significant systematic error.

Our Monte Carlo (MC) simulations are now performed as follows. The size of the simulation box size was set to 48^3 for a total of 105984 nematic particles, excluding the boundary

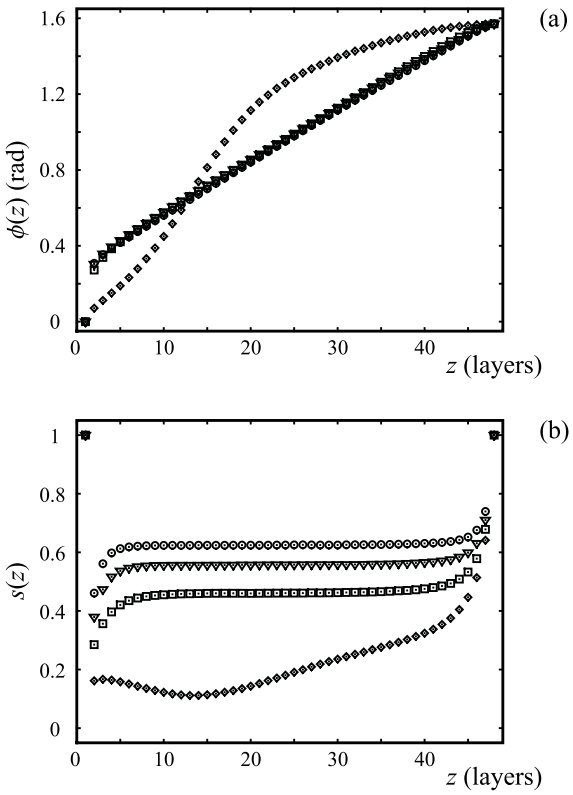


FIG. 2: Hybrid cell with smooth substrates and $\nu = 0$ (external anchoring at $z = 0$): director (a) and order parameter (b) profiles for $T^* = 1.50$, 1.42, 1.34, and 1.26 (diamonds, squares, triangles, and circles, respectively); the bulk NI transition temperature approaches $T^*_{NI} \approx 1.52$.

particles $\mathbf{p}_i$ in the layers at $z = 0$ and $z = d$. In case of disordered substrates particle orientations in the confining layers are generated following a probability distribution $f(\phi) \propto \exp(-\mathcal{P}\cos^2\phi)$, which gives a homeotropic easy axis ($\phi = 0$) and a $\mathcal{P}$-dependent degree of order S_0. For example, $\mathcal{P} \to 0$ corresponds to a distribution close to isotropic, while $\mathcal{P} \to \infty$ yields a perfectly aligned substrate. Then, the hexagonal lattice is divided into three sublattices, as shown in Fig. 1, ensuring that the bonds between neighboring particles on the lattice never connect two particles from the same sublattice. Considering the simple hexagonal lattice as tripartite enables us to vectorize the simulation algorithm, which provides a significant speed-up in calculations. Further, in the x and y directions periodic boundary conditions are assumed. We start either from a random configuration in two dimensions (recall that $\mathbf{u}_i$ are restricted to lie in hexagonal planes), or from an equilibrated configuration at a temperature slightly higher than the simulated one, if this is available.

Then we apply the standard Metropolis algorithm [23]. For our vectorized algorithm to work correctly, in each MC cycle we first attempt (and accept/reject) trial moves involving particles in the first sublattice and only then proceed to the second one, and after that to the third one. In generating a new trial configuration each time only a single particle is involved. We have typically performed 10^5 MC cycles for equilibration, followed by 10^5 production cycles to accumulate averages of interest.

We measure the extrapolation length by analyzing the director profile $\phi(z)$. The $\phi(z)$ dependence is calculated by accumulating the two independent components of the two–dimensional ordering matrix $Q_{\alpha\beta}(z) = 2\langle u_i^\alpha u_i^\beta \rangle_z - \delta_{\alpha\beta}$, where α and β can be either x or z, and u_i^α represents the α component of the unit vector $\mathbf{u}_i$. The average $\langle ... \rangle_z$ is performed both over all particles in the layer centered at z and over the production MC cycles. Then, the averaged ordering matrix is diagonalized and the positive eigenvalue is identified as the two–dimensional scalar order parameter $s(z)$. Accordingly, the corresponding eigenvector is the director. Note that in Ref. [16] the extrapolation length in the LL model with three–dimensional spins was studied, using a different method to obtain the director profile. Rather than computing the ordering matrix, the polar angle averaged over all particles in a layer and over production MC cycles was computed; i.e., no information was kept about the azimuthal orientation of the particles. This method overestimates the actual average director tilt angle for small values of this angle. The strong temperature dependence of the extrapolation length found in Ref. [16] is most likely an artifact of the incorrect method used in that paper.

III. EXTERNAL ANCHORING

We analyze the spatially isotropic intermolecular interaction first by setting $\nu = 0$ in Eq. (1). Such a model is now similar to the standard LL model, yet it is characterized by a different coordination number (eight in the former model, six in the latter) and the dimensionality of nematic spins (two in the former model, three in the latter). These distinctions lead to a different balance between the decrease of internal energy and loss of orientational entropy upon going from the isotropic into the nematic phase, and thus shift the NI transition to a temperature higher than in the LL model. Monitoring temperature scans of internal energy, specific heat, and the order parameter s (lowercase s will be used throughout the

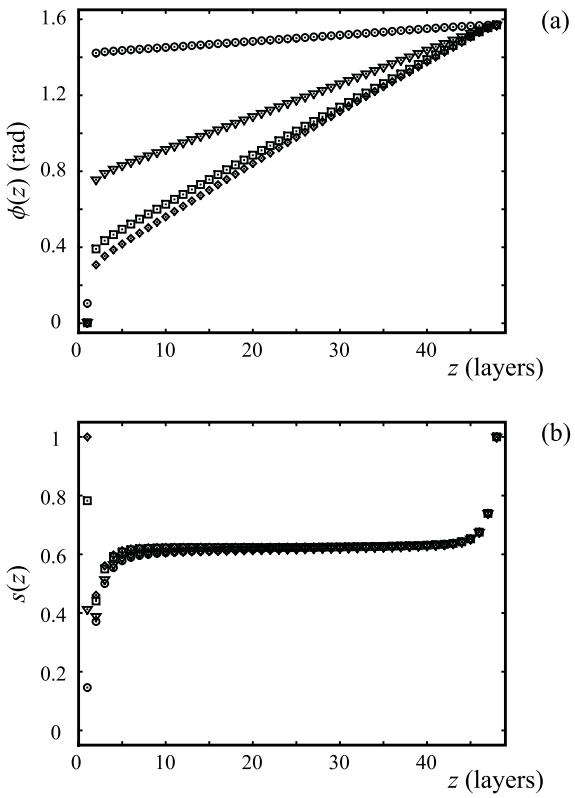


FIG. 3: Hybrid cell with a rough homeotropic substrate at $z = 0$: director (a) and order parameter (b) profiles for $\nu = 0$, $T^* = 1.26$, and different degrees of substrate roughness s_0. Circles, triangles, squares, and diamonds correspond to $s_0 = 1$, $s_0 \approx 0.78$, $s_0 \approx 0.41$, and $s_0 \approx 0.15$, respectively.

text for the two–dimensional order parameter), for $\nu = 0$ we estimate the dimensionless transition temperature in a 48^3 bulk sample (with full periodic boundary conditions) to be $T^*_{NI} = k_B T_{NI}/\epsilon \approx 1.52 \pm 0.01$. Here a dimensionless temperature scale, $T^* = k_B T/\epsilon$, has been introduced.

Consider the director and order parameter profiles [$\phi(z)$ and $s(z)$, respectively] in a hybrid nematic cell where both substrates are smooth and hence impose perfect nematic order with $s_0 = 1$. Recall that for $\nu = 0$ one is dealing exclusively with external anchoring. Fig. 2(a) shows $\phi(z)$ profiles for different temperatures. One can readily observe that far enough from the NI transition the profiles approach a linear function (predicted also from Frank elastic theory [5]), with minor changes in slope $|d\phi/dz|$ only close to substrates where the degree of order can vary. In particular, wherever $s(z)$ exceeds its bulk value s_b, the nematic

becomes more difficult to deform, which results in a reduction in slope (and vice versa). Moreover, note that far enough from the NI transition [in our simulations for values of reduced temperature $\tau = (T^*_{NI} - T^*)/T^*_{NI} \gtrsim 0.07$] the $\phi(z)$ profiles are essentially insensitive to changing temperature. Given $w = 0.1$, as chosen above for the homeotropically anchored smooth left wall, the extrapolation length is estimated as $b = 11.6a(1 \pm 7\%)$, where a is the lattice spacing. Significant deviations from the linear $\phi(z)$ profile can be observed only close to T^*_{NI} [for $\tau \lesssim 0.02$], when the nematic far enough from the walls melts and thereby avoids elastic distortion — see Fig. 2 (b). Then molecular alignment becomes homeotropic in the vicinity of the left surface, followed by a region of (nearly) isotropic liquid in the slab center, and by a region of planar alignment close to the right surface. Note that one can avoid this nematic "meltdown" by reducing the deformation strength, e.g., by setting $0 < \phi(d) \ll \pi/2$ or by reducing w at the $z = d$ wall. In this case b is observed to be essentially T^*-independent even up to $\tau \approx 0.02$. Note, however, that thereby the immediate vicinity of the NI transition actually has not been probed: for a realistic liquid crystal with $T_{NI} \approx 300$ K, $\tau \approx 0.02$ corresponds to temperatures as much as 6 K below the transition. Alternatively, the deformation strength can be reduced also by significantly increasing the system size. Further, in Fig. 2 (b) one can always observe an increase of s when approaching the substrate at $z = d$ promoting planar alignment. Similarly, s decreases close to the $z = 0$ substrate because of a weaker nematic–substrate coupling ($w = 0.1$ as opposed to $w = 1$ for the $z = d$ substrate).

Turn now to cases with a rough homeotropic substrate, simulated by generating an ensemble of fixed particles $\mathbf{p}_i$ at $z = 0$ with $s_0 < 1$. Qualitatively, the behavior of $\phi(z)$ and $s(z)$ does not change, including the insensitivity of b to variations of T^* in the temperature range presently accessible. However, as shown in Fig. 3 for $T^* = 1.26$, a smaller s_0 reflects in a reduced anchoring strength at $z = 0$ and hence in a reduced slope $|d\phi/dz|$, which, in turn, results in a larger b: for $s_0 \approx 0.78$ we find $b = 14.9a(1 \pm 7\%)$, for $s_0 \approx 0.41$, $b = 31a(1 \pm 7\%)$, and for $s_0 \approx 0.15$, $b = 50a(1 \pm 48\%)$ (for a summary see Table I). Note that in the latter case b already approaches the sample thickness d and is already close to violating the stability condition $d \gtrsim b$ for the deformed director structure [21]. Moreover, assuming $K \propto s_b^2$ and $W \propto s_0 s(0)$, the extrapolation length should scale as $b \propto s_b^2/s(0)s_0$. The full quantitative agreement, however, turns out to be rather poor (even within error bars).

Note that in the vicinity of fairly disordered substrates the nematic becomes elastically

TABLE I: Extrapolation lengths b measured in units of lattice spacing a: substrate roughness-dependence for external anchoring ($\nu = 0$) and values for intrinsic anchoring ($\nu \neq 0$), together with the corresponding dimensionless bulk NI phase transition temperatures T^*_{NI}. The values are given for $T^* \lesssim 1.42$ ($\nu = 0$), $T^* \lesssim 1.265$ ($\nu = 0.05$), and $T^* \lesssim 1.13$ ($\nu = 0.1$), i.e., for $\tau \gtrsim 0.07$, where b is essentially temperature-independent.

ν	T^*_{NI}	anchoring	s_0	b (a)
0	1.52 ± 0.01	external	1.0	$11.6\,(1 \pm 7\%)$
			0.78	$14.9\,(1 \pm 7\%)$
			0.41	$31\,(1 \pm 7\%)$
			0.15	$50\,(1 \pm 48\%)$
0.05	1.36 ± 0.01	intrinsic		$16.3\,(1 \pm 13\%)$
0.1	1.21 ± 0.01	intrinsic		$4.6\,(1 \pm 10\%)$

softer than in the bulk, which increases the local slope of the director profile $\phi(z)$ in comparison with the bulk. As the NI transition is approached, the thickness of this disordered layer ($\sim \xi$) starts to grow, thereby indirectly affecting the bulk slope of $\phi(z)$, which — in principle — could result in a more pronounced temperature dependence for b that is extrapolated from the bulk. Note, however, that a significantly thicker sample than the present one is required to actually observe this scenario.

We also studied the influence of the hexagonal lattice structure and the confinement of $\mathbf{u}_i$ to the xz plane on our results, by analyzing external anchoring in the original LL model where the spins $\mathbf{u}_i$ are three–dimensional vectors. Both the LL and hexagonal lattice models yield the same qualitative behavior: a nearly temperature-independent b which increases in value as the surface roughness is increased.

IV. INTRINSIC ANCHORING

Setting $\nu \neq 0$, intrinsic anchoring appears at the interfaces, in addition to the external contribution present already for $\nu = 0$. Note that changing ν affects not only anchoring, but also changes the elastic softness of the nematic [24]: for ν not too large ($\nu \lesssim 0.78$), the

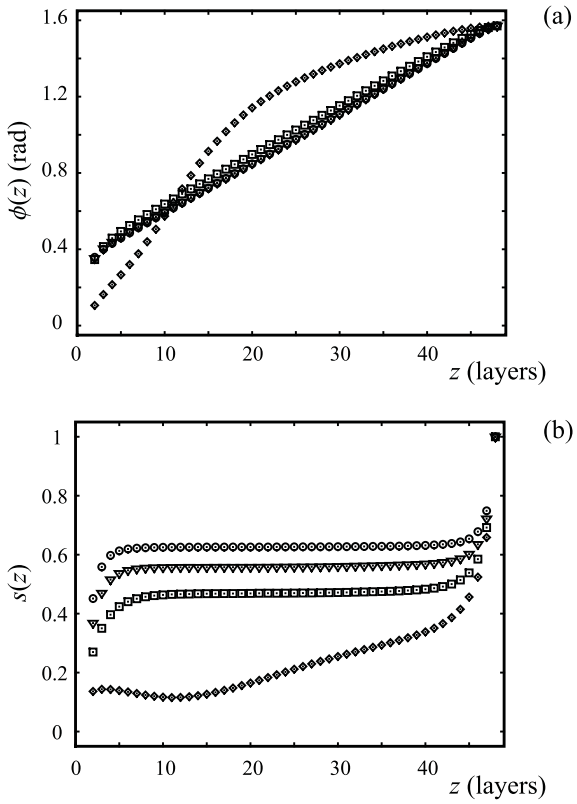


FIG. 4: Nematic slab with a single free interface at $z = 0$ and $\nu = 0.05$ (homeotropic intrinsic anchoring). Same profiles as in Fig. 2, yet for rescaled values of T^*: $T^* = 1.335$, 1.265, 1.195, and 1.125 (diamonds, squares, triangles, and circles, respectively). $T^*_{NI} \approx 1.36$.

Frank elastic constant decreases with increasing ν. Consequently, upon increasing ν, the NI transition temperature is found to decrease (see Table I). Therefore, when comparing b for different values of ν, it is appropriate to rescale the temperature T^* and compare measurements with comparable values of the reduced temperature τ (resulting in similar values of s_b).

To facilitate the analysis, we decided to remove the wall at $z = 0$ allowing us to deal with intrinsic anchoring alone. When $\nu \lesssim 0.3$ (but nonzero) the intrinsic easy axis remains homeotropic [11], and the hybrid cell-like geometry studied in the previous section is maintained. As in the case of pure external anchoring, we find that the intrinsic extrapolation length b shows no temperature dependence (within estimated error; see Fig. 4). However, b does depend on the anisotropy of the nematic-nematic interparticle potential: for $\nu = 0.05$ and $\nu = 0.1$ one finds $b = 16.3a(1 \pm 13\%)$ and $b = 4.6a(1 \pm 10\%)$, respectively (see Table I

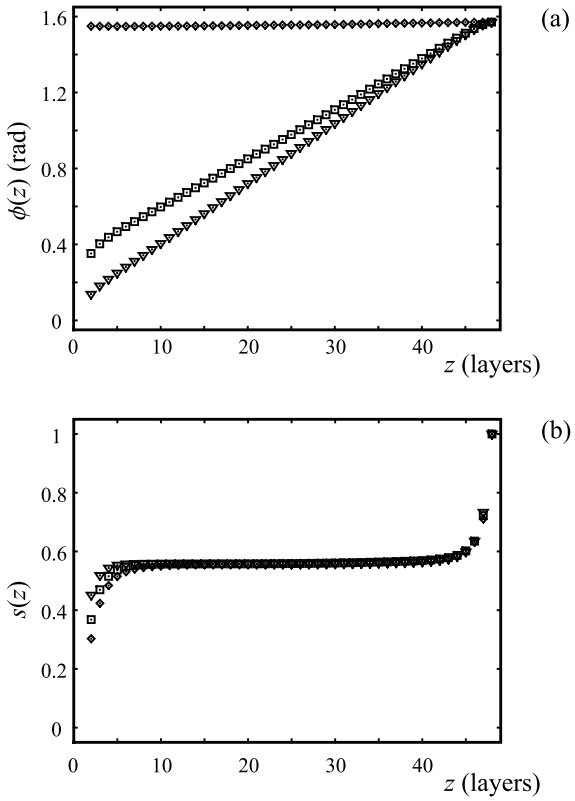


FIG. 5: Same as Fig. 4, but for different values of the bulk interaction anisotropy: $\nu = 0$, $\nu = 0.05$, and $\nu = 0.1$ (diamonds, squares and triangles, respectively). The corresponding temperatures are $T^* = 1.34$, $T^* = 1.195$, and $T^* = 1.065$, respectively, ensuring that the bulk value of the order parameter and the reduced temperature be the same in all cases ($\tau \approx 0.12$). There is no intrinsic anchoring for $\nu = 0$, while for $\nu \neq 0$ an increase of ν results in a decrease of the extrapolation length.

and Fig. 5). This trend can be attributed to an increase of the anchoring energy W, as well as to a simultaneous decrease of the elastic constant K upon increasing ν. Note that in the analysis of Ref. [11] $b = 8a(1 \pm 13\%)$ was found for $\nu = 0.1$ at zero temperature. The disagreement with the current largely temperature–independent estimate can be attributed to considering only nearest neighbors in the present analysis, which — as already stated — results in an underestimation of b.

Note, moreover, that for $\nu > 0.1$ extrapolation lengths are in the microscopic range (of the order of a few — up to 5 — lattice spacings a). On the other hand, experimental values of the extrapolation length are typically of the order of 100 nm or greater [9]. We can obtain

quantitative agreement between our results and experiments by a significant decrease of the ν parameter, as also suggested in Ref. [11]. A small value of ν in Eq. (1) promotes parallel alignment, as is favored, e.g., by steric repulsions in a system of hard rods. A decrease in ν might therefore be regarded as an effective inclusion of steric repulsions which are absent in our lattice model.

V. CONCLUSIONS

In this paper we have studied the anchoring of a nematic liquid crystal to a solid substrate and to a free interface, using numerical simulations of a simple hexagonal lattice model of two–dimensional spins interacting through a spatially anisotropic potential. We focused on the roles of substrate roughness and of the spatial anisotropy of the interparticle potential. An elastic deformation was imposed on the simulation cell, allowing us to extract the surface extrapolation length b from the director profile. Setting the anisotropy of the potential to zero allowed us to probe the strength of the external anchoring (the anchoring arising from the direct interaction of the nematic with the surface). For temperatures not too close to the nematic–isotropic transition the extrapolation length was found to be largely temperature independent, and to grow with increasing surface roughness (as characterized by the distribution of the local preferred axis on the surface). This increase is physically reasonable, reflecting the decrease in the overall anchoring of the nematic as the surface becomes more disordered. Qualitatively similar behavior was found when we simulated the original Lebwohl–Lasher model where the spins are three–dimensional.

With the full anisotropic interaction potential present, intrinsic anchoring arises due to the incomplete spin–spin interactions at the sample surface. For a free nematic interface (and external anchoring absent), we extracted the intrinsic surface extrapolation length. Like the extrapolation length in the presence of only external anchoring, this length is temperature–independent. We found that the strength of the intrinsic anchoring grows together with the elastic softness of the nematic as the interaction potential anisotropy is increased, leading to smaller values of the extrapolation length. Thus, obtaining agreement with the experimentally measured values of b, on the order of 100 nm, requires a relatively small value of the interaction anisotropy parameter ν approaching 10^{-2}.

Acknowledgments

Computational work in support of this research was performed at the Theoretical Physics Computing Facility at Brown University. Financial support from the National Science Foundation under Grant Nos. INT–9815313 and DMR–0131573, and from the Slovenian Office of Science (Programmes No. P0-0503-1554 and 0524-0106) is gratefully acknowledged.

---

[1] G. P. Crawford and S. Žumer, *Liquid Crystals in Complex Geometries Formed by Polymer and Porous Networks*, (Taylor and Francis, London 1996).

[2] A. Rapini and M. Papoular, J. Phys. (Paris) Colloq. **30,** C4–54 (1969).

[3] K. Okano, Jpn. J. Appl. Phys. **22,** L343 (1983).

[4] A. Mertelj and M. Čopič, Phys. Rev. Lett. **81,** 5844 (1998).

[5] P. G. de Gennes and J. Prost, *The Physics of Liquid Crystals* (Clarendon, Oxford 1993).

[6] D. J. Cleaver and M. P. Allen, Phys. Rev. A **43,** 1918 (1991).

[7] D. Andrienko, G. Germano, and M. P. Allen, Phys. Rev. E **62,** 6688 (2000).

[8] M. Nobili and G. Durand, Phys. Rev. A **46,** R6174 (1992).

[9] L. M. Blinov, A. Yu. Kabayenkov, and A. A. Sonin, Liq. Cryst. **5,** 654 (1989).

[10] L. R. Evangelista and S. Ponti, Phys. Lett. A **197,** 55 (1995).

[11] G. Skačej, V. M. Pergamenshchik, A. L. Alexe-Ionescu, G. Barbero, and S. Žumer, Phys. Rev. E **56,** 571 (1997).

[12] A. P. J. Emerson, S. Faetti, and C. Zannoni, Chem. Phys. Lett. **271,** 241 (1997).

[13] S. J. Mills, C. M. Care, M. P. Neal, and D. J. Cleaver, Phys. Rev. E **58,** 3284 (1998).

[14] M. A. Bates and C. Zannoni, Chem. Phys. Lett. **280,** 40 (1997).

[15] M. P. Allen, Mol. Phys. **96,** 1391 (1999).

[16] N. Priezjev and R. A. Pelcovits, Phys. Rev. E **62,** 6734 (2000).

[17] M. Bates, Phys. Rev. E **65,** 041706 (2002).

[18] P. A. Lebwohl and G. Lasher, Phys. Rev. A **6,** 426 (1972); **7,** 2222 (E) (1973).

[19] W. Maier and A. Saupe, Z. Naturforsch. A **14,** 882 (1959); **15,** 287 (1960);

[20] J.Nehring and A. Saupe, J. Chem. Phys. **54,** 337 (1971); **56,** 5527 (1972).

[21] G. Barbero and R. Barberi, J. Phys. (Paris) **44,** 609 (1983).

[22] C. Chiccoli, P. Pasini, A. Šarlah, C. Zannoni, and S. Žumer, to appear in Phys. Rev. E.

[23] N. Metropolis, A. W. Rosenbluth, M. N. Rosenbluth, A. H. Teller, and E. Teller, J. Chem. Phys. **21,** 1087 (1953).

[24] G. Barbero, Mol. Cryst. Liq. Cryst. **195,** 199 (1991).